US Army Corps
of Engineers
Hydrologic Engineering Center

Identifying the Probability Distribution of Precipitation Annual Maxima for Probabilistic Flood Hazard Analysis

Implications of Gumbel's Extreme Value Theory

August 2020

TP-163

REPORT DOCUMENTATION PAGE

Form Approved OMB No. 0704-0188

1. REPORT DATE *(DD-MM-YYYY)*	2. REPORT TYPE	3. DATES COVERED *(From - To)*
August 2020	Technical Paper	

4. TITLE AND SUBTITLE
Identifying the Probability Distribution of Precipitation Annual Maxima for Probabilistic Flood Hazard Analysis: Implications of Gumbel's Extreme Value Theory

5a. CONTRACT NUMBER

5b. GRANT NUMBER

5c. PROGRAM ELEMENT NUMBER

6. AUTHOR(S)
Gregory S. Karlovits, U.S. Army Corps of Engineers
Melvin G. Schaefer, MGS Engineering Consultants

5d. PROJECT NUMBER

5e. TASK NUMBER

5F. WORK UNIT NUMBER

7. PERFORMING ORGANIZATION NAME(S) AND ADDRESS(ES)
US Army Corps of Engineers
Institute for Water Resources
Hydrologic Engineering Center (CEIWR-HEC)
609 Second Street
Davis, CA 95616-4687

8. PERFORMING ORGANIZATION REPORT NUMBER
TP-163

9. SPONSORING/MONITORING AGENCY NAME(S) AND ADDRESS(ES)

10. SPONSOR/ MONITOR'S ACRONYM(S)

11. SPONSOR/ MONITOR'S REPORT NUMBER(S)

12. DISTRIBUTION / AVAILABILITY STATEMENT
Approved for public release; distribution is unlimited.

13. SUPPLEMENTARY NOTES

14. ABSTRACT

Gumbel's extreme value theory is examined in light of L-moments technology and the L-Moment Ratio Diagram (LMRD) for the case of precipitation annual maxima. Identification of the probability distribution for precipitation annual maxima for a specific homogeneous storm type is an important task in the development of a watershed precipitation-frequency relationship for use in stochastic flood modeling for Risk-Informed Decision-Making (RIDM). Convergence to the Generalized Extreme Value (GEV) distribution behaves systematically for parent probability distributions with L-skewness and L-kurtosis pairings that reside above or below the GEV curve on the LMRD. Specifically, precipitation Peak-Over-Threshold (POT) datasets representing parent distributions for various storm types converge to the GEV distribution from below the GEV curve on the LMRD. The degree of convergence, nearness to GEV, is dependent upon the number of storm events per year from which the annual maxima are drawn and the mathematical form of the parent distribution. The four-parameter Kappa distribution provides a convenient mathematical form for the usual case where the resultant probability distribution for precipitation annual maxima is near, but has not yet converged to the GEV distribution.

15. SUBJECT TERMS
Gumbel, extreme value theory, L-moments, regional frequency analysis, probability distribution, storm typing

16. SECURITY CLASSIFICATION OF:			17. LIMITATION OF ABSTRACT	18. NUMBER OF PAGES	19a. NAME OF RESPONSIBLE PERSON
a. REPORT	b. ABSTRACT	c. THIS PAGE			19b. TELEPHONE NUMBER
U	U	U	UU	20	

Identifying the Probability Distribution of Precipitation Annual Maxima for Probabilistic Flood Hazard Analysis

Implications of Gumbel's Extreme Value Theory

August 2020

US Army Corps of Engineers
Institute for Water Resources
Hydrologic Engineering Center
609 Second Street
Davis, CA 95616

(530) 756-1104
(530) 756-8250 FAX
www.hec.usace.army.mil

TP-163

Papers in this series have resulted from technical activities of the Hydrologic Engineering Center (HEC). Versions of some of these have been published in technical journals or in conference proceedings. The purpose of this series is to make the information available for use in HEC's training program and for distribution with the U.S. Army Corps of Engineers (USACE).

The findings in this report are not to be construed as an official Department of the Army position unless so designated by other authorized documents.

The contents of this report are not to be used for advertising, publication, or promotional purposes. Citation of trade names does not constitute an official endorsement or approval of the use of such commercial products.

Identifying the Probability Distribution of Precipitation Annual Maxima for Probabilistic Flood Hazard Analysis

Implications of Gumbel's Extreme Value Theory

Introduction

Identification of the best-fit probability distribution for precipitation annual maxima for a specified storm type is an important task in the development of a site-specific watershed precipitation-frequency (PF) relationship for use in stochastic flood modeling (Carney et al., 2018; Nathan et al., 2003, 2016; Schaefer & Barker, 2005; SEFM, 1998; Smith et al., 2015). L-moments (Hosking, 1990) are typically used to identify the regional probability distribution for point precipitation for a specified storm type as part of a regional PF analysis (Hosking & Wallis, 1997; L-RAP, 2005; Schaefer et al., 2016).

Stochastic flood modeling is a common method for performing a detailed Probabilistic Flood Hazard Analysis (PFHA) to assess hydrologic risk at federally-owned dams in the United States and at major water projects in Australia. The findings from the PFHA provide probabilistic hydrologic loadings as inputs to risk analysis for use in Risk-Informed Decision-Making (RIDM). An aspect of stochastic flood modeling that distinguishes this application from other flood-frequency analyses is the need to have precipitation and flood estimates for extreme Annual Exceedance Probabilities (AEPs) in the range of 10^{-3} to 10^{-7}. The design of large hydraulic infrastructure typically employs the estimated limiting value (ELV) principle (Chow et al., 1988) which implies extremely small AEP events for capacity exceedance, e.g., dam overtopping. Flood estimates at these extreme AEPs are required because of the potential for loss-of-life and high economic damages resulting from a failure of a large dam.

A key element of the stochastic approach is the development of the watershed PF relationship. The shape of the watershed PF relationship is dependent upon several factors including: storm type; point precipitation L-moment statistics; probability distribution for point precipitation; temporal storm characteristics for the specified storm type; and the spatial storm characteristics relative to the geometric shape of the watershed of interest (Alexander, 1963; Fontaine & Potter, 1989; Foufoula-Georgiou, 1989; Schaefer et al., 2016; Schaefer 2017a, 2017b). Figure 1 depicts a watershed PF relationship and uncertainty bounds for the mid-latitude cyclone (MLC) storm type for the Cherokee Dam watershed in the Tennessee Valley, located in Eastern Tennessee, USA. This watershed PF relationship was developed using a stochastic storm generation procedure (Schaefer, 2017b) that included point precipitation findings (MGS Engineering et al., 2015) obtained from regional PF analysis and the spatial correlation structure for the synoptic scale mid-latitude cyclone storm type. The Tennessee Valley study also displayed that uncertainty in the selected probability distribution for point precipitation, along with uncertainty in the regional L-skewness measure, are typically the primary contributors to the total uncertainty variance (Figure 2) for extreme AEPs in the range of 10^{-3} to 10^{-7}. Thus, identification

of the regional probability distribution for point precipitation is a critical task in the development of a watershed PF relationship for stochastic flood modeling.

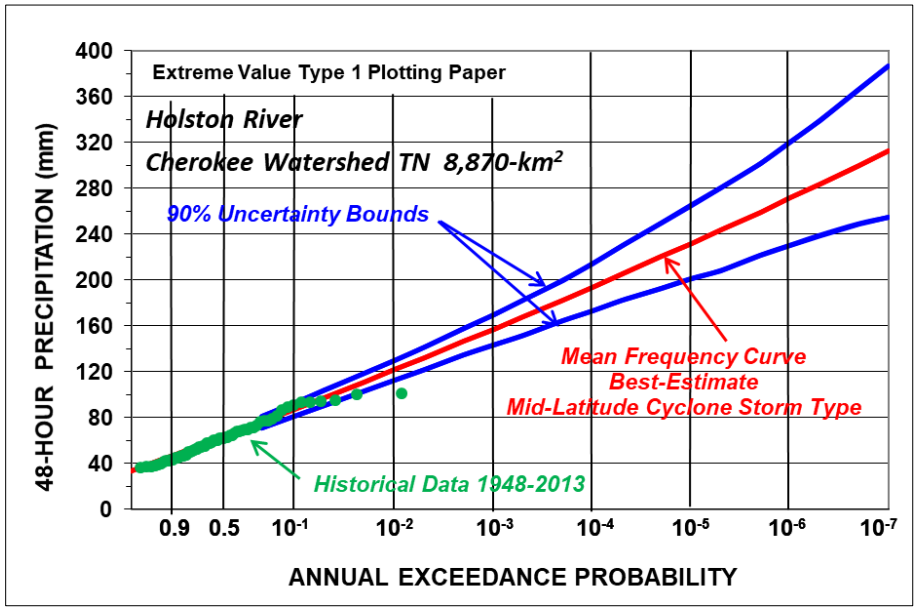

Figure 1. Example of watershed precipitation-frequency (PF) relationship and 90% uncertainty bounds for the mid-latitude cyclone (MLC) storm type for the Cherokee Dam Watershed, Tennessee.

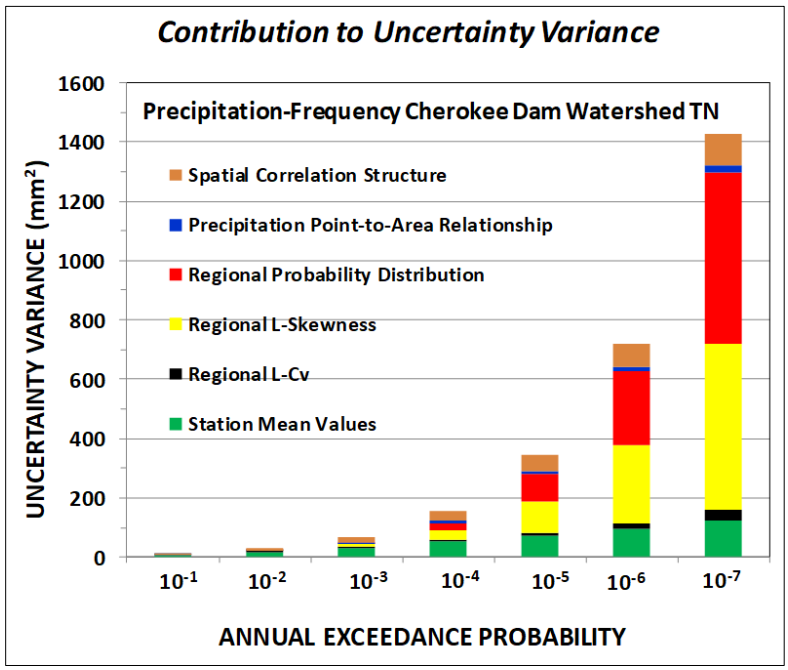

Figure 2. Example of relative contribution of various sources of uncertainty to total uncertainty variance for watershed precipitation-frequency (PF) relationship for mid-latitude cyclone (MLC) storm type for Cherokee Dam Watershed, Tennessee.

The recent implementation of storm typing (MGS Engineering et al., 2015), for assembling precipitation annual maxima datasets for regional PF analysis, produces greater homogeneity regarding the physical and statistical behavior of specific storm types. In this context, storm types may be generally categorized in North America as: synoptic scale mid-latitude cyclone (MLC); synoptic scale tropical storm and tropical storm remnant (TSR), mesoscale storm with embedded convection (MEC); and local storm (LS). Our experience has been that use of the nominal 48 hour, 6 hour, and 2 hour durations have been representative of the period during which the majority of precipitation occurs for the synoptic-scale, mesoscale and local storm types in North America.

Recent experiences with storm typing procedures within L-moment based regional PF analyses, for several large regions within the United States (MetStat et al., 2018a and b; MGS Engineering et al., 2014), have resulted in a new perspective on Gumbel's original work on extreme value statistics (Gumbel, 1958). The intent of this paper is to reconcile recent observations of convergence behavior of block maxima of properly homogenized populations with the underlying theory of extreme value statistics. The agreement of theoretical and observed convergence of point precipitation extremes has major implications affecting regional PF analysis; further, this convergence behavior can assist in identification of a regional probability distribution for point precipitation annual maxima.

This paper will discuss the development of the field of extreme value theory and its relevance to precipitation-frequency analyses, demonstrate how the behavior of extremes for meteorologically-homogeneous datasets across North America can be predicted using classical extreme value theory, utilize Monte Carlo simulation to investigate the convergence properties of homogeneous samples, and recommend a probability distribution useful for modelling incomplete convergence of extremes.

Gumbel Convergence Theory and L-Moments

Extreme value theory underpins the general framework for performing PF analyses. Extreme value theory is a field with a long and rich history, with its discovery generally credited to Fréchet (1927), Fisher and Tippett (1928), Gumbel (1935), and Gnedenko (1943). For studies of block maxima, generally the annual maximum from a parent population, the first extreme value theorem is of most importance. This theorem, named the Fisher-Tippett-Gnedenko theorem, states that properly normalized maxima of independent and identically distributed (iid) random variables converge in distribution to one of three asymptotic forms (see Equation (1), summarizing Gnedenko (1943)):

$$c_n^{-1}(M_n - d_n) \xrightarrow{d} \begin{cases} \Lambda(x) \\ \Phi(x) \\ \Psi(x) \end{cases} \quad \textbf{(1)}$$

where Λ, Φ and Ψ are the three asymptotic forms of extreme value distribution.

For a sequence of iid random variables $X_1, X_2, \ldots, X_n$ with common distribution function F, and $M_n = \max\{X_1, \ldots, X_n\}$; of interest is the distribution of the maximum M_n. An exact distribution $\Pr(M_n \leq z)$ arises from the joint probability of not exceeding the z magnitude of the extreme

event in each of the n random variables; $\Pr(M_n \leq z) = \Pr(X_1 \leq z, \ldots, X_n \leq z)$ and due to independence $\Pr(M_n \leq z) = \Pr(X_1 \leq z) * \Pr(X_2 \leq z) * \ldots * \Pr(X_n \leq z) = \big(F(z)\big)^n$. For scale parameter $c_n > 0$ and location parameter $d_n \in \mathbb{R}$, which normalize M_n, convergence in the distribution (e.g., Resnick, 2010) occurs. This convergence is analogous to the central limit theorem (CLT), except analyzing the maxima of a sample instead of the sample mean. In the CLT, usage the normalizing term d_n is the population mean and c_n the population standard deviation divided by the root of the sample size n. The asymptotic form is the standard normal distribution.

Practically, F and the normalization constants c_n and d_n are rarely known or of concern, because analysis begins with block maxima, and the form and parameters of the asymptotic result are used directly. Furthermore, the maxima convergence to one of the three limiting forms is dependent on the underlying population F. Gumbel's 1958 unifying monograph *Statistics of Extremes* detailed the asymptotic distributions to which various forms of F converge. These three distributional forms are the extreme value (EV) types I, II and III (Gnedenko's Λ, Φ and Ψ, respectively). For the case of block maxima that have positive values of the data, EV type I (EV1) is a two-parameter distribution called by Gumbel the "double exponential distribution" and was later named in his honor; it has no lower or upper bound. EV type II (EV2) is a three-parameter distribution, which has a lower bound and no upper bound and is referred to as the Fréchet distribution. EV type III (EV3) is a three-parameter distribution, which has an upper bound and is named for the Swedish mathematician Waloddi Weibull.

Groupings of the mathematical forms of F whose block maxima converge to one of the three extreme value distributions is said to fall in that distribution's maximum domain of attraction (MDA) (Embrechts et al., 1997). Broadly speaking, F belonging to the exponential family of distributions fall into the Gumbel MDA. F with heavy tails (called the "Cauchy" form by Gumbel, in some literature, e.g., Goldie & Resnick (1988), the sub-exponential family) fall into the Fréchet MDA. Finally, F with lighter than exponential tails, or a fixed upper bound (called the "limited" form by Gumbel), fall into the Weibull MDA.

Block maxima are constructed from sequential samples of maxima taken from non-overlapping "blocks" of a parent process (for hydrologic applications, generally the maximum event per water year). Such treatment is usually in the interest of collecting an iid sample of severe events. For PF analyses, the underlying process from which the maxima are drawn creates zero or more events per block (year). The rate of convergence of the distribution of the maxima to one of the three asymptotic forms is based on both the properties of the process as well as the number of events per block from which the maxima are drawn. Incomplete convergence to the asymptotic form occurs for multiple reasons: principally, the generally slow rate of convergence for some forms of F and norming constants c_n and d_n, and the limited number of events that occur in each block from which the maxima might be drawn (Embrechts et al., 1997). The behavior of the convergence of the block maxima described above will be termed Gumbel Convergence Theory for convenience in this paper.

In the field of hydrometeorology, the adoption of the Generalized Extreme Value (GEV) distribution, which subsumes the EV types I, II and III, is generally due to Jenkinson (1955, 1969). Each subtype is represented with the GEV shape parameter κ with $\kappa < 0$ for EV2, $\kappa > 0$ for EV3, and $\kappa = 0$ for EV1. The GEV distribution has myriad parameterizations, but the authors

choose to employ the Hosking location-scale-shape parameterization (Hosking et al., 1985) for its consistency in interpretation of the parameters of the GEV, Generalized Pareto, and Generalized Logistic distributions. The inverse cumulative distribution function (quantile function $F^{-1}(p)$) for the GEV distribution has the mathematical form (see Equation (2)):

$$F^{-1}(p|\xi,\alpha,\kappa) = \xi + \frac{\alpha}{\kappa}\{1 - [-log(p)]^{\kappa}\} \quad \kappa \neq 0$$
$$F^{-1}(p|\xi,\alpha) = \xi - \alpha log[-log(p)] \quad \kappa = 0 \qquad \textbf{(2)}$$

where: ξ, α, κ are location, scale, and shape parameters, respectively.

L-moments provide a robust method for computing sample statistics, characterizing the shapes of probability distributions and for fitting of distribution parameters for selected probability distributions within the framework of a regional frequency analysis. L-moment descriptions of sample characteristics tend to be less sensitive to outliers than conventional product moments (Vogel & Fennessey, 1993). The L-moments L-location, L-CV, L-skewness, and L-kurtosis have similar application and utility as the moment-based counterparts of the mean, and coefficients of variance, skewness, and kurtosis, respectively. The L-moment Ratio Diagram (LMRD) provides a convenient graphic for displaying the relationship between L-skewness and L-kurtosis for probability distributions as well as sample data. On the LMRD, two-parameter distributions have fixed L-skewness and L-kurtosis and display as points, three-parameter distributions have L-kurtosis dependent on L-skewness and display as lines, and four or more parameter distributions are shown as regions. Figure 3 depicts the range of the LMRD and several probability distributions useful for PF analyses and are listed in the figure.

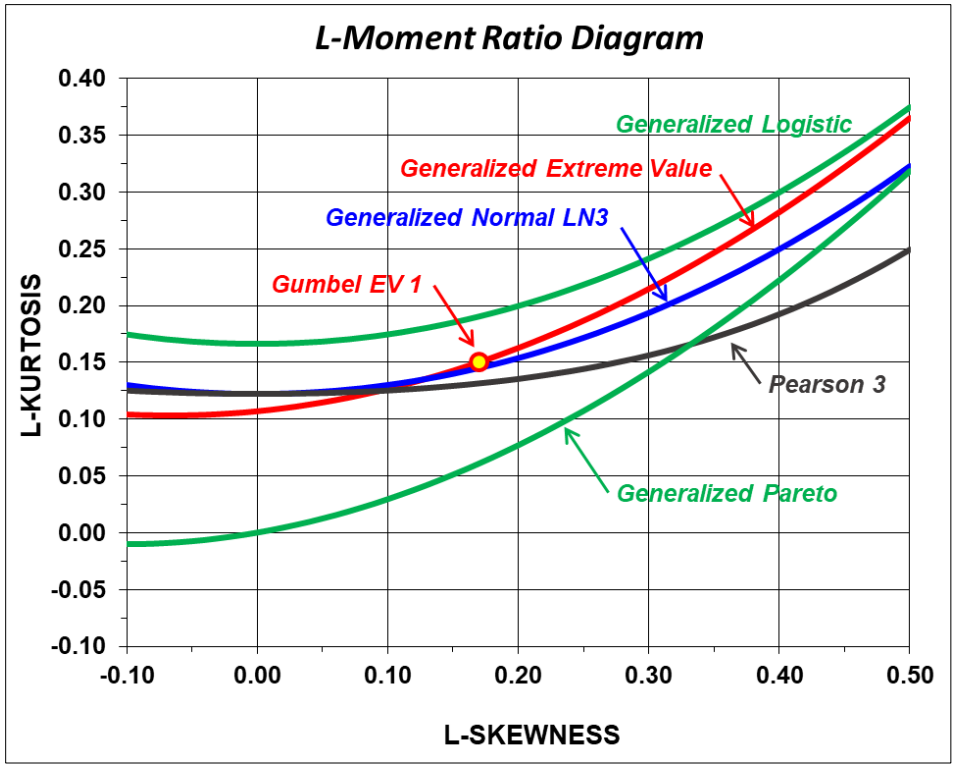

Figure 3. L-Moment Ratio Diagram (LMRD) displaying L-skewness versus L-kurtosis relationships for selected three-parameter probability distributions.

The MDA for various combinations of population L-skewness and L-kurtosis are depicted on the LMRD in Figure 4. Populations with L-skewness-L-kurtosis pairings below the black line fall into the Weibull MDA; populations along the black line the Gumbel MDA; and populations above the black line the Fréchet MDA. The MDA for maxima from a probability distribution can change depending on parameter values for flexible distributions, which often have one or more parameters that affect the tail weight and support of the distribution.

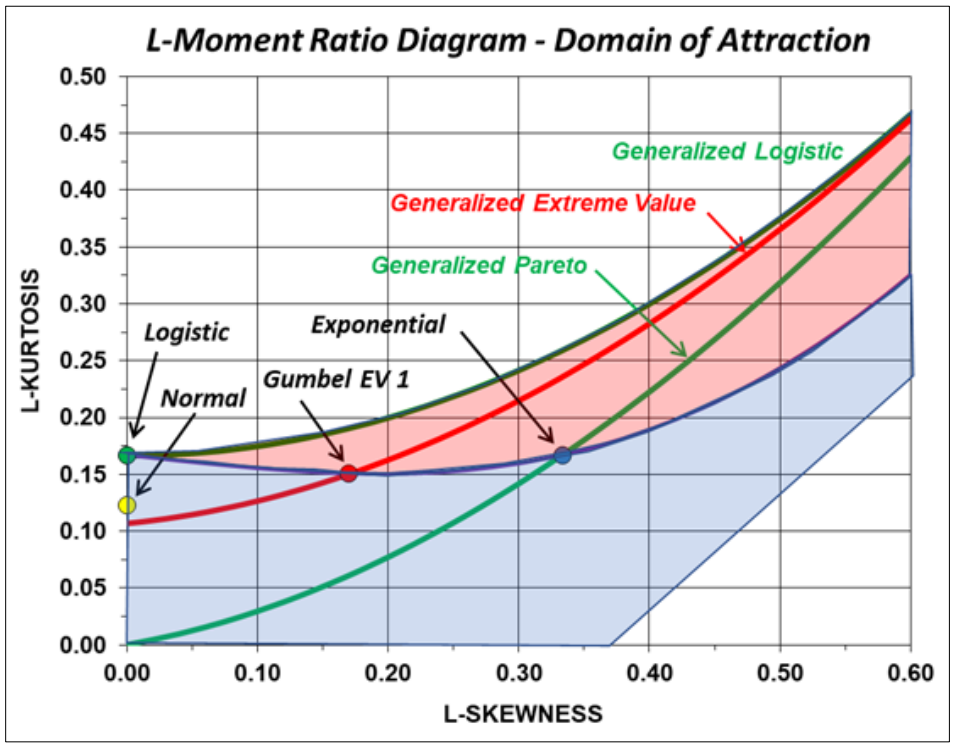

Figure 4. L-Moment Ratio Diagram (LMRD) displaying the maximum domain of attraction (MDA) for selected parent populations (red = Fréchet MDA, blue = Weibull MDA, black line = Gumbel MDA).

Experience with Regional Precipitation Datasets using Storm Typing

Findings from recent large-area regional PF studies (Table 1) for the Western Sierra Mountains California (Schaefer & Barker, 2005), and the states of Tennessee (MGS Engineering, 2014), Texas (MetStat 2018a), and Colorado – New Mexico (MetStat 2018b) indicated the regional probability distribution for point precipitation is near the GEV distribution for humid climates where a given storm type occurs many times each year. Indeed, this is a common situation for the MLC storm type in a humid climate as illustrated in Figure 5 where the LMRD plot displays the L-skewness and L-kurtosis pairings for 38 homogeneous sub-regions in the Tennessee Valley study area (MGS Engineering, 2014). Moreover, the sampling distributions for L-skewness and L-kurtosis are nearly normally distributed, and the scatter in the data (due to the large number of stations and samples in the region) asymptotically approach a bivariate Normal distribution (Hosking & Wallis 1997). The centroid of the sub-region data for the MLC example plots just below the GEV curve.

Table 1. Sample Sizes for Regional Annual Maxima Datasets for Various Storm Types.

Study Area	LMRD Figure	Storm Type[1]	Duration (hr)	Homogeneous sub-regions	Number of stations	Station-years of record
Tennessee Valley	Figure 5	MLC	48	38	794	46,393
Colorado – New Mexico	Figure 6	LS	2	10	84	3,039
Texas	Figure 7	TSR	48	33	650	15,341

[1]**Refers to the figure in this paper.**

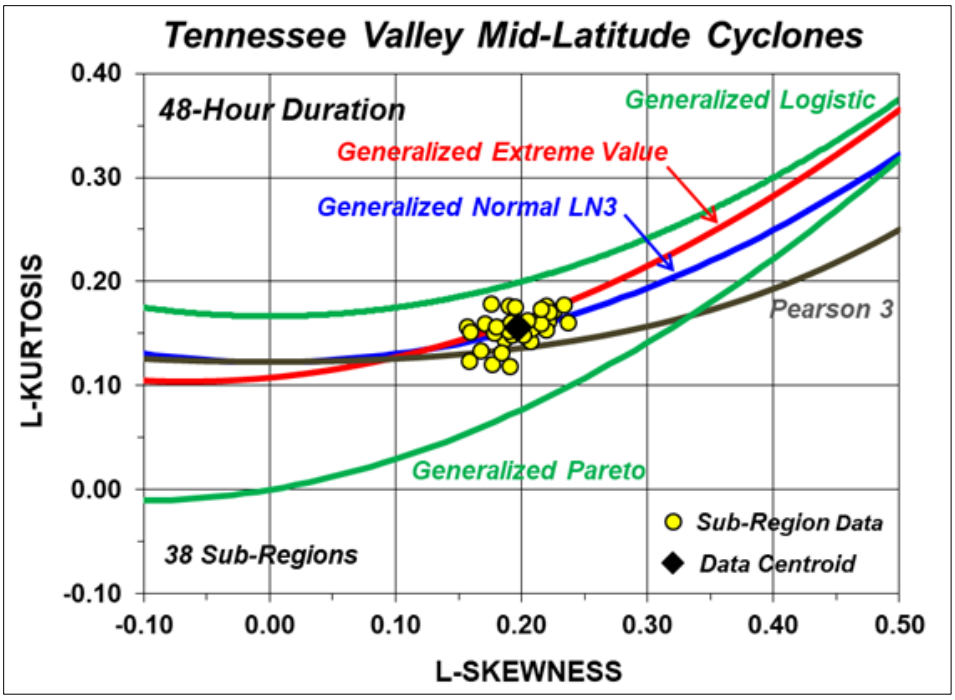

Figure 5. L-skewness - L-kurtosis pairings for homogeneous sub-regions in the Tennessee Valley study area for the mid-latitude cyclone (MLC) storm type.

Conversely, in arid and sub-arid climates where a given storm type produces few storms in any given year, the identified probability distribution commonly plots on the LMRD further below the GEV curve. The LMRD plot presented in Figure 6 depicts the L-skewness and L-kurtosis pairings for 10 homogeneous sub-regions in the inter-mountain semi-arid western Colorado-New Mexico study (MetStat et al., 2018b) for the LS convective storm type. Further, the data cluster and centroid of the L-skewness and L-kurtosis pairings is clearly below the GEV curve. Thus, the spread in L-skewness values is associated with climatic conditions where arid areas have greater L-skewness relative to semi-arid and sub-humid environments. If the GEV distribution were selected for the LS storm type in the Colorado-New Mexico study area, it would result in quantile estimates being overestimated, particularly for extreme AEPs.

Regional PF analysis for precipitation produced in coastal areas exclusively by tropical storms was not possible until 2014 (MGS Engineering 2014) when storm typing was first employed in a PFHA context for assembly of annual maxima precipitation datasets for the TSR storm type. TSR events do not occur every year at some coastal sites, and in some years the TSR precipitation is too small to be representative of the TSR phenomenon. Therefore, this situation requires using a mixed discrete-continuous distribution with a mixing parameter describing the fraction of years with little or no TSR precipitation (a probability mass at zero) and a probability

distribution describing TSR precipitation that exceeds a frequency-based threshold (continuous distribution) (MGS 2015). This TSR method was applied to events in the Texas study area (Table 1).

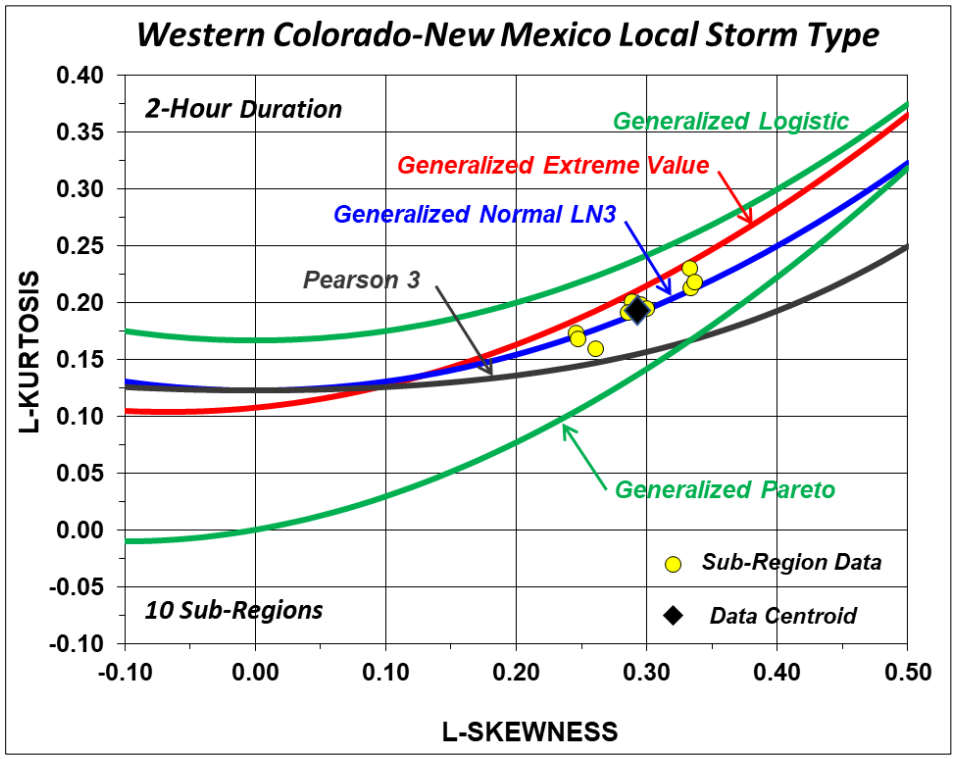

Figure 6. L-skewness - L-kurtosis pairings for homogeneous sub-regions in the Western Colorado-New Mexico study area for the local storm (LS) storm type.

Figure 7 depicts the L-skewness and L-kurtosis pairings for 33 homogeneous sub-regions in the coastal and central areas of Texas with data for those years when a TSR event was recorded at the individual stations (MetStat et al., 2018a). Distinctively, the data cluster and centroid of the L-skewness and L-kurtosis pairings is clearly seen to be well below the GEV curve and near the Generalized Pareto (GPA) distribution. The sub-region data are seen to parallel the GPA curve, where greater L-skewness values are associated with distance from the coast and drier climatic conditions further inland from the coast. The nearness of the sub-region data to the GPA curve is consistent with the situation where only one or a few TSR events occur in a year and the resultant probability distribution for the annual maxima has not moved far from the parent probability distribution. Collectively, Figure 5 (MLC), Figure 6 (LS), and Figure 7 (TSR) depict three distinct cases for the effect of the number of storm events per year and convergence toward the GEV distribution from below.

Storm typing produces a distinct benefit in PF analyses, namely in strengthening the assumption of independent and identically-distributed populations (iid) from which block maxima are drawn. Homogenization of these iid populations allows for better characterization of the parent population and leads to stronger implications regarding the terminal convergence of block maxima sampling toward the GEV distribution. With storm-typed populations representing a homogenous sample of a meteorological process, the MDA to which the parent belongs might be

more readily identified, which affects estimates for parameter uncertainty for the distribution of maxima drawn from that population.

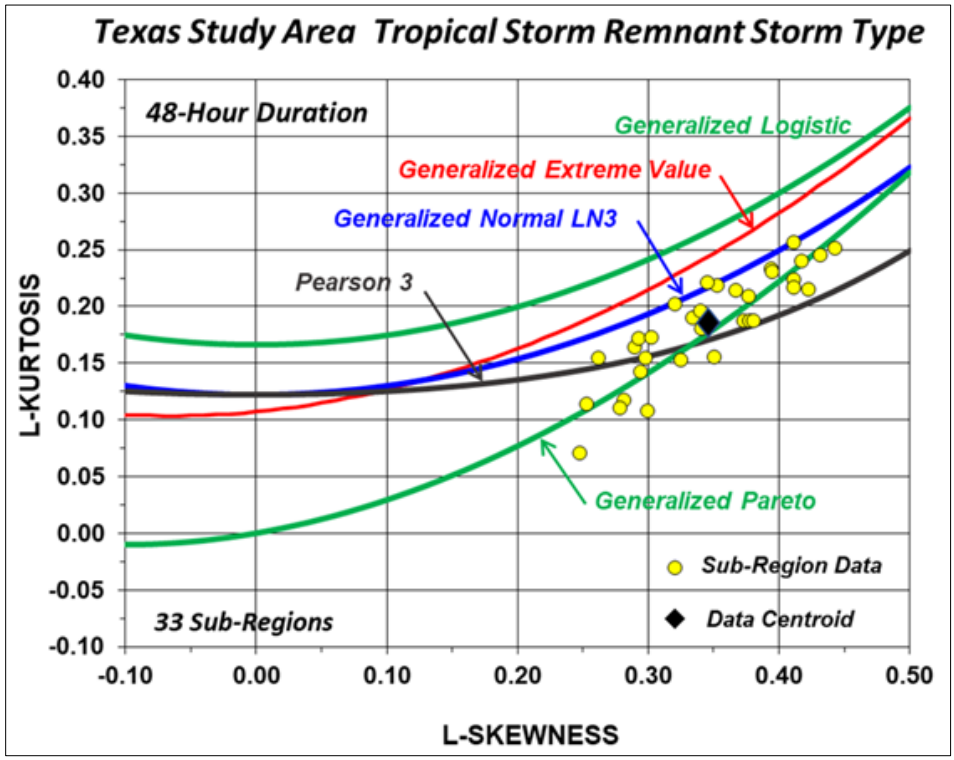

Figure 7. L-skewness - L-kurtosis pairings for homogeneous sub-regions in the Texas study area for the tropical storm remnant (TSR) storm type.

Simulations of Gumbel Convergence for Selected Parent Probability Distributions

Monte Carlo simulations for a variety of probability distributions and distribution parameter combinations were used to examine Gumbel Convergence behavior regarding the number of events per year from which the annual maximum was obtained. The simulations were conducted with a sample size of 500 annual maxima for a given scenario of the parent distribution and distribution parameters, and 100 scenarios were conducted for each of a preselected number of events per sample year to reduce the effects of sampling variability. To show convergence to GEV the number of events simulated per sample year were 1, 2, 3, 4, 5, 6, 8, 10, 15, 20, 30, 40, 60, 80 and 100.

Figure 8 shows that when the parent distribution resides above the GEV curve on the LMRD, the L-moment ratios for L-skewness and L-kurtosis and associated probability distribution converge to the GEV distribution from above and from left to right. There are three examples in Figure 8 for cases where the three-parameter Generalized Logistic (GLO) distribution is the parent distribution, with varying L-skewness. In addition, a Wakeby-distributed parent is shown with a very large value of L-kurtosis that converges to GEV when the annual maximum is selected from just 5 events per year. All four of the parent distributions with high L-kurtosis demonstrate the same trajectory of convergence to GEV from above, and from left to right.

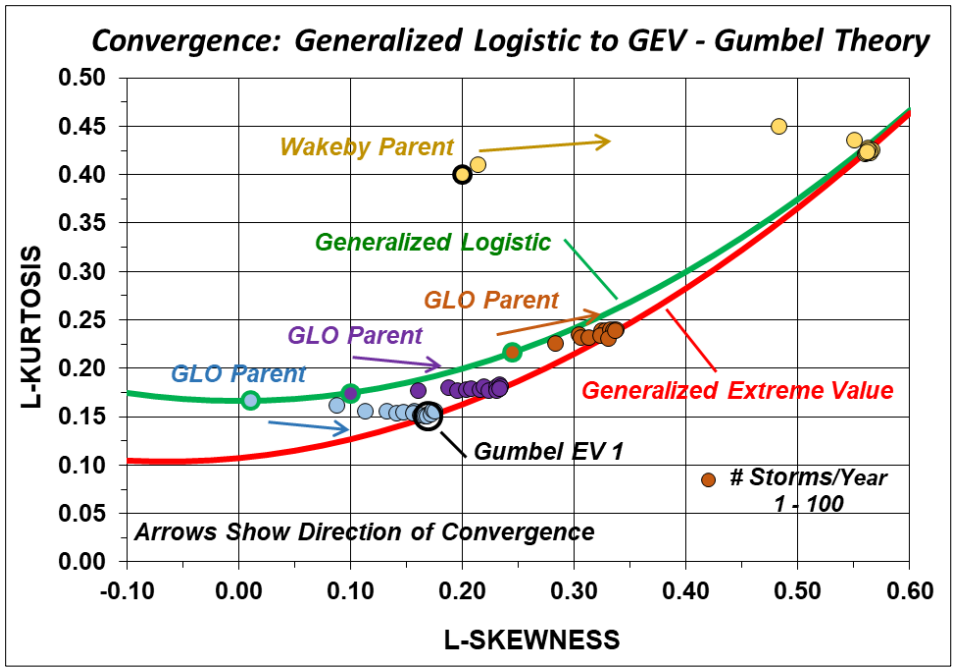

Figure 8. Progression of convergence from the three Generalized Logistic (GLO) distribution examples and the Wakeby distribution to the Generalized Extreme Value (GEV) distribution as a function of the number of events (1-100) from which annual maxima are selected.

Conversely, when the parent distribution resides below the GEV curve, convergence to the GEV distribution occurs from below and from right to left. Figure 9 depicts examples for convergence from the GPA parent distribution with varying L-skewness to the GEV distribution. In both the GLO and GPA cases, the Monte Carlo results have heavy upper tails and the rate of convergence is relatively quick with fewer than 10 events per year needed to get near the GEV distribution.

The last set of examples is for the Pearson type 3 (PE3) distribution (Figure 10) which converges to the Gumbel EV1 distribution because the Gamma distribution, of which the PE3 is a generalization, falls into the exponential family of probability distributions. For the case of L-skewness = 0.01, which is nearly normally distributed, convergence to the Gumbel EV1 distribution has not quite occurred even with the annual maxima chosen from 100 events per sample year. This outcome is due to the very light upper tail for L-skewness = 0.0100, as well as the relatively slow convergence of all samples in the Gumbel MDA (Resnick, 1986).

Beyond the convergence behavior of sample L-skewness and L-kurtosis is that the lower order L-moments also vary with the number of storm events per year in progressing from the parent distribution to the GEV distribution. Figure 11 depicts the change in the L-location, L-CV, L-skewness, and L-kurtosis for the case of the GPA distribution with a mean of 1.0, L-CV = 0.3, L-skewness = 0.4 and L-kurtosis = 0.22. This systematic behavior in the population moments demonstrates the anticipated increase in central tendency and reduction in variation consistent with the impact of the sample size on the norming constants (see for example Embrechts et al., 1997).

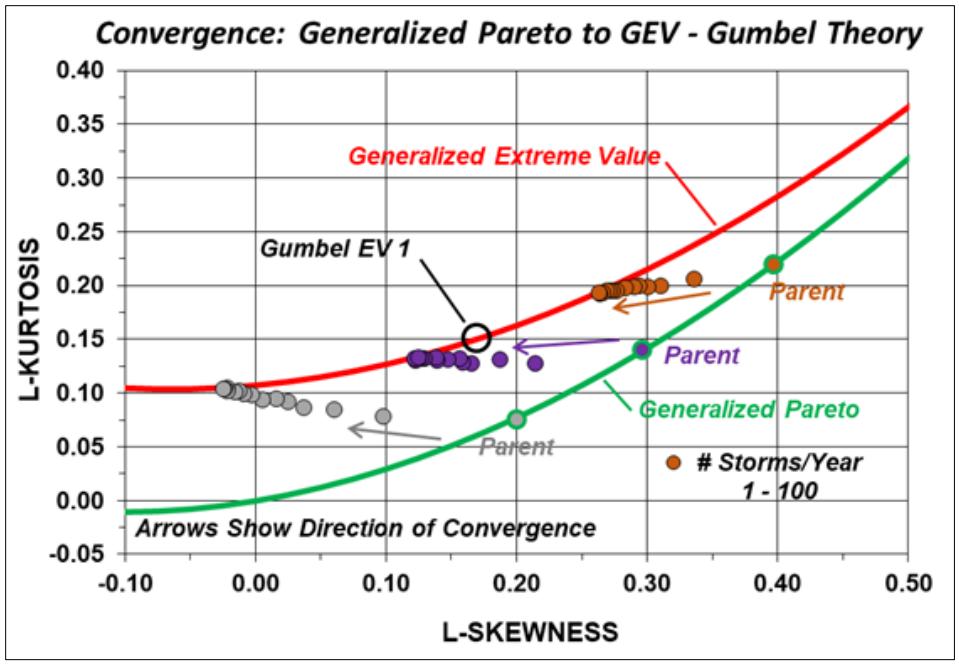

Figure 9. Progression of convergence from the three Generalized Pareto (GPA) distribution examples to the Generalized Extreme Value (GEV) distribution as a function of the number of events (1-100) from which annual maxima are selected.

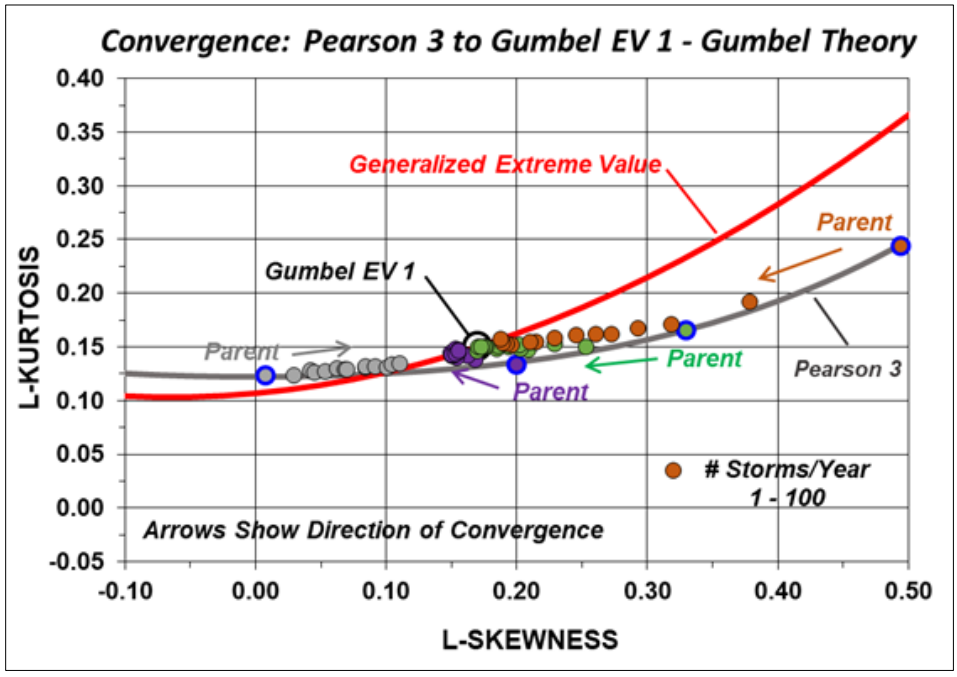

Figure 10. Progression of convergence from four Pearson type 3 distribution examples to the Gumbel extreme value type 1 (EV1) distribution as a function of the number of events (1-100) from which annual maxima are selected.

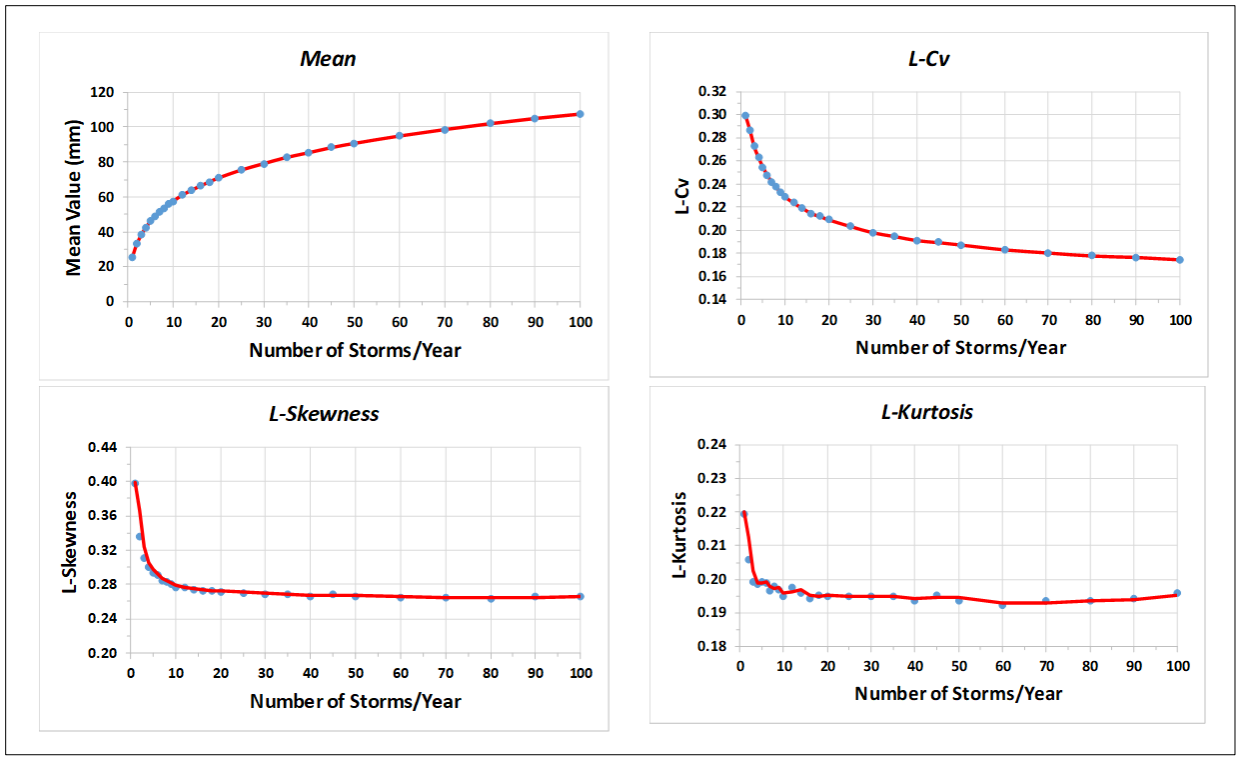

Figure 11. Variation of L-moments with number of storm events per year from which annual maximum is chosen for Generalized Pareto (GPA) parent distribution example.

Examples of Parent Probability Distributions for Selected Storm Types and Locations

Datasets for representative parent distributions for selected storm types and locations were assembled to assess the Gumbel convergence behavior specifically for meteorologically-homogenous precipitation datasets. Peak-Over-Threshold (POT) datasets were assembled for long-term, high-quality hourly precipitation stations in the U.S. for storm types and durations where meteorologists have indicated that a given storm type signature is strong. Thresholds were selected based on meteorological judgment of the smallest value that is reasonably representative of the storm type of interest at a given location. Thresholds generally resulted in a rate of occurrence between about three and nine events per year, which was judged sufficiently frequent to be representative of a parent distribution in arid to humid climates, respectively. Table 2 lists the locations and durations for the various storm types and Figure 12 depicts the location of sample L-skewness and L-kurtosis pairings on the LMRD. In addition, Figure 7 shows L-skewness and L-kurtosis pairings for homogeneous sub-regions for the TSR storm type. Due to the small number of TSR events per year, the pairings are near to the parent distribution, which is distinctly different from the GEV distribution.

A review of Figure 7 (for TSR type) and Figure 12 (for other storm types) shows all L-skewness and L-kurtosis pairings for the four storm types to be plotting below the GEV curve and generally in the parameter space between the GEV and GPA distributions. Results for the individual stations are at-site samples subject to sampling variability. Nonetheless, these

L-skewness and L-kurtosis pairings are consistent with prior experience and conventional practice (Stedinger et al., 1993) that precipitation annual maxima datasets, for durations less than several days (individual storm events), are generally well described by the GEV distribution and precipitation POT datasets are generally well-described by the GPA distribution. The latter result is a natural example of the second extreme value theorem, also called the Pickands-Balkema-de Haan theorem (Balkema & de Haan 1974, Pickands 1975), which is concerned with the distribution of samples exceeding a selected threshold. Samples constructed by POT converge to the GPA much in the same way that block maxima converge to the GEV distribution, and this behavior plays a role in explaining the observed convergence towards the GEV distribution in meteorologically-homogenous regions of point precipitation samples.

Table 2. Precipitation Stations Used for Assembling Peak-Over-Threshold Precipitation Datasets for Selected Storm Types.

Stn ID	Station Name	State	Storm Type	Duration (hr)	Threshold (mm)	Events per year	Years of record	Sample L-skewness	Sample L-kurtosis
040897	Blue Canyon WSO	CA	MLC	48	68.6	7.0	60	0.357	0.231
311690	Charlotte WSO AP	NC	MLC	48	27.9	8.0	64	0.337	0.207
052220	Denver WBFO AP	CO	MLC	48	7.4	7.0	61	0.433	0.267
404950	Knoxville WSO AP	TN	MLC	48	30.7	8.0	64	0.381	0.210
356751	Portland WB AP	OR	MLC	48	25.1	9.0	62	0.336	0.214
457781	Snoqualmie Pass	WA	MLC	48	66.0	9.0	57	0.318	0.186
090451	Atlanta WSO AP	GA	MEC	6	19.3	8.0	65	0.374	0.205
311690	Charlotte WSO AP	NC	MEC	6	17.5	8.0	65	0.348	0.194
401656	Chattanooga WSO	TN	MEC	6	18.3	8.0	64	0.387	0.224
111549	Chicago O'Hare WSO	IL	MEC	6	17.0	8.0	51	0.381	0.242
118179	Springfield WSO AP	IL	MEC	6	16.0	8.0	65	0.379	0.226
111549	Chicago O'Hare WSO	IL	LS	2	11.4	8.0	51	0.399	0.228
052220	Denver WBFO AP	CO	LS	2	7.6	5.0	61	0.412	0.202
266779	Reno WSFO AP	NV	LS	2	4.1	4.0	64	0.410	0.272
118179	Springfield WSO AP	IL	LS	2	11.2	8.0	65	0.360	0.210
048832	Tehachapi Rangr Stn	CA	LS	2	2.5	2.5	61	0.525	0.283

Information about the parent distribution and the number of events per year for these homogeneous regions provide insight into the nearness of the resultant probability distribution to the GEV distribution for annual maxima. This information is particularly useful because of the importance of identification of the probability distribution (Figure 2) when computing quantile estimates of extreme AEPs.

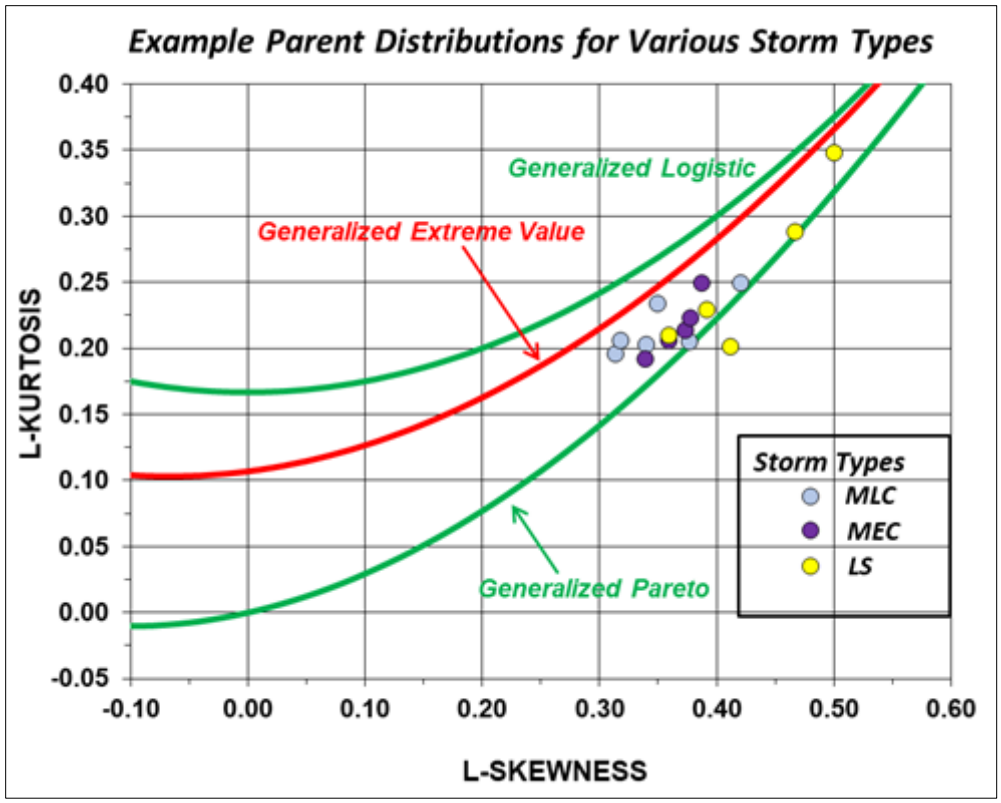

Figure 12. L-skewness and L-kurtosis Pairings for precipitation peak-over-threshold datasets for various storm types observed at locations in the United States.

Sampling Variability and Data Quality Issues

The experience gained in conducting numerous regional analyses shows that it is not uncommon to find sub-regional pairings of L-skewness and L-kurtosis above the GEV curve. We have seen this occur for a variety of reasons. For example, in Figure 5 the sub-regional values above the GEV curve are the result of sampling variability, which would be anticipated with a population value shown at the centroid point on the LMRD near the GEV line. In addition, sub-regional solutions for L-skew and L-kurtosis can also be affected by extreme observations that are unrepresentative of the sample size used in their estimation. Our experience has been that final regional solutions residing above the GEV curve are often associated with incomplete quality checking of datasets that have false annual maxima for low values associated with incomplete records. Homogeneity of the sampling with regard to storm typing is also a critical piece. Moreover, surrogates for meteorological storm typing, such as filtering by seasonality and/or duration, may be inadequate for ensuring that the parent populations are sufficiently homogeneous. Therefore, studies that only employ these strategies, for example Karlovits et al., (2017) or Schaefer and Barker (2005), can result in annual maximum distributions slightly above the GEV curve.

Identification of Probability Distribution for Precipitation Annual Maxima

As shown above, POT datasets with a low threshold are representative of a parent distribution in the context of applying Gumbel Convergence Theory for precipitation annual maxima. In addition, prior investigation (Stedinger et al., 1993) has shown the GPA distribution to be a reasonable choice for POT analyses of precipitation maxima for individual storm events with durations from several minutes to several days. These conditions indicate the parent probability distribution for precipitation maxima resides below the GEV curve on the LMRD. Application of Gumbel Convergence Theory therefore, yields convergence towards the GEV distribution from below the GEV curve. Finally, the large-area regional studies summarized in Table 1, and example stations listed in Table 2, demonstrate that extreme precipitation samples constructed from homogenous populations have parent populations on the GPA side of the GEV curve of the LMRD, not the GLO side.

There are several important implications of this situation.

1. The GEV curve on the LMRD creates an upper bound on distributional choices for precipitation annual maxima for durations associated with individual storm events.

2. In climatic environments where there are a small number of storm events of a given storm type each year, it is reasonable to expect that the probability distribution for annual maxima for that storm type has not converged to the GEV distribution.

3. If quantile estimates for extreme AEPs are of interest, then a probability distribution in the distributional space below the GEV curve on the LMRD that can replicate the observed annual maxima data should be selected to model the population.

Large-area regional precipitation-frequency (PF) studies conducted using storm typing procedures should produce further observations of the convergence of homogeneous region PF distributions toward the GEV distribution. The collection of results from studies past and future potentially lead to the application of Bayesian techniques based on prior information available for estimation of L-moment ratios and the level of convergence to the GEV distribution. This approach can be used to produce reasonable results for screening level hydrologic risk analyses without requiring extensive detailed analyses for the PF component.

Advantages of Four-Parameter Kappa Distribution for Precipitation Annual Maxima

The four-parameter Kappa distribution (Hosking, 1994) is applicable over a large parameter space on the LMRD ranging from a second shape parameter (h) value of -1 to infinity (Figure 13). This characteristic makes this distribution a logical choice for the regional probability distribution for point precipitation for developing a watershed PF relationship for use in stochastic flood modeling as part of a PFHA.

Equation (3) shows the quantile function ($F^{-1}(p)$) for the four-parameter Kappa distribution:

$$F^{-1}(p|\xi,\alpha,\kappa,h) = \xi + \frac{\alpha}{\kappa}\left\{1 - \left(\frac{1-p^h}{h}\right)^k\right\} \quad \textbf{(3)}$$

where: ξ, α, κ, and h are location, scale and two shape parameters, respectively; and p is the cumulative probability. The cases $h = 0$ and $k = 0$ are implicitly continuous limits.

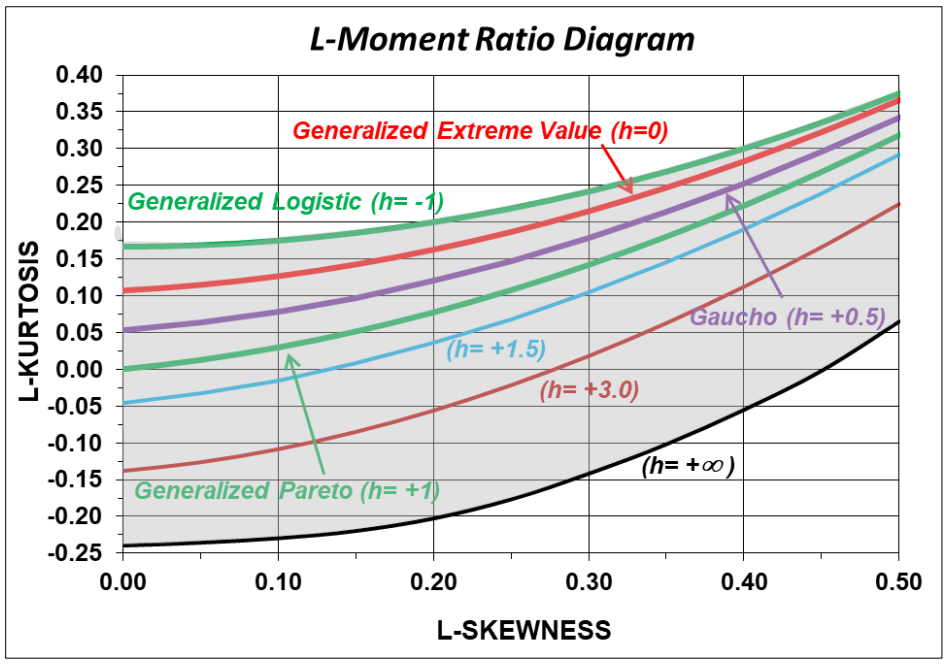

Figure 13. L-skewness and L-kurtosis parameter space applicable to four-parameter Kappa distribution.

Several conventional three-parameter distributions are special cases of the Kappa distribution, distinguished by the value of the second shape parameter h. These include the GLO (h = -1), GEV (h = 0), Gaucho (h = +0.5, Nunez et al., 2011) and GPA (h = +1). In this context, these three-parameter distributions can be envisioned as a four-parameter Kappa distribution with a fixed value for the second shape parameter h. This feature makes the Kappa distribution attractive for describing precipitation annual maxima, and allows uncertainties in identification of the regional probability distribution to be simulated by varying h. The utility of the h parameter can also be viewed from the perspective of Gumbel Convergence Theory where the h parameter, as fitted by the method of L-moments, varies with the number of storms per year. Figure 14 provides the change in the h parameter with the number of storms per year for the GPA example parent distribution with L-skewness = 0.400 displayed in Figure 11.

In practice, the centroids of the data clusters shown in Figure 5, Figure 6, and Figure 7 would be fitted by the four-parameter Kappa distribution where a fixed h value effectively results in a three-parameter distribution.

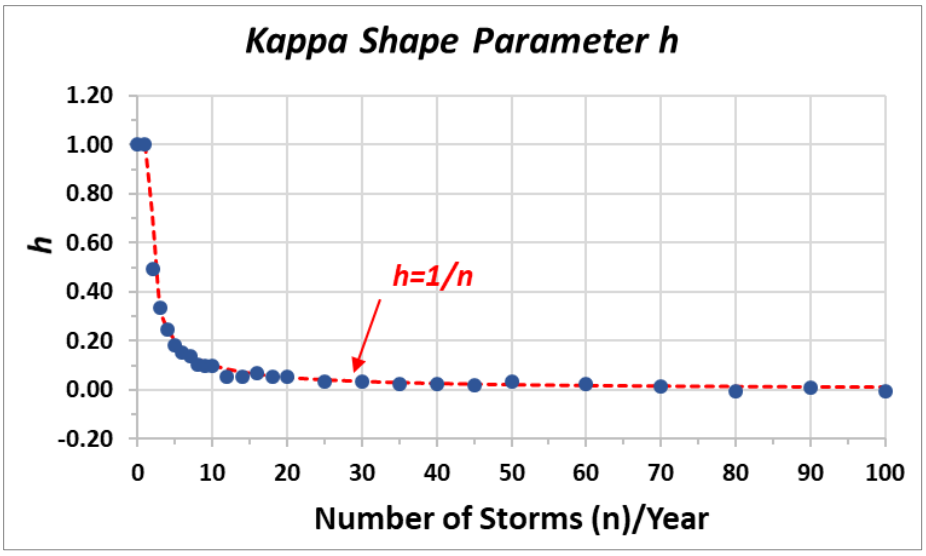

Figure 14. Variation of the second shape parameter h of the four-parameter Kappa distribution with the number of storm events per year from which the annual maximum is chosen for a Generalized Pareto (GPA) parent distribution example.

Use of the Kappa Distribution is also consistent with the trajectory of sample convergence as seen in Figure 9 for the GPA distribution. Convergence occurs along "iso-kappa" lines, which are lines of equal value of the Kappa distribution's first shape parameter (κ). This is a result consistent with the formulation of the Hosking location-scale-shape GLO, GEV, and GPA distributions (Hosking, 1994). These iso-kappa lines establish two points: identification of the GEV sub-distribution to which the parent distribution would eventually converge with enough events per year; and a regionally-based estimator for the annual maximum Kappa distribution's first shape parameter κ based on the homogenous parent population. This result is also consistent with the observation in equality of the shape parameter of the GEV and GPA distributions for block maxima taken from a GPA population made by Hosking and Wallis (1987). Additionally, Hosking (1994) showed that the maximum of a binomially-distributed count of GPA samples has a Kappa distribution with $h = 1/n$, which is consistent with the simulation results shown in Figure 14. Finally, the location and scale parameters of the Kappa distribution (ξ and α) are consistent with the GEV location and scale parameters derived from a parent GPA as shown by Madsen et al., (1997, review equations 10 and 11).

Figure 15 displays the iso-kappa trajectory of convergence of a parent GPA with $\kappa = 0.077$ which converges to an EV3 distribution, and the trajectory for the GPA example in Figure 9 with $\kappa = -0.143$ which converges to an EV2 distribution. Furthermore, the sample maximum simulated L-moments for 1 to 100 events per year (yellow circles) are shown in Figure 15 for comparison with the $\kappa = -0.143$ iso-kappa line.

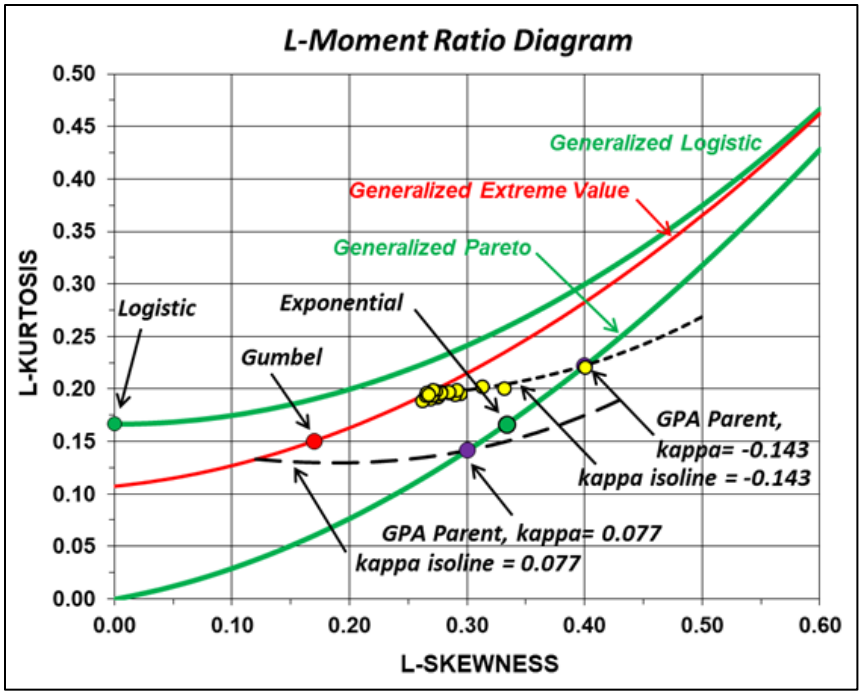

Figure 15. Example iso-kappa lines of convergence for two Generalized Pareto (GPA) parents, with the sample maximum simulated L-moments for number of events per year (1-100).

Addressing Uncertainties in Identification of Probability Distribution for Precipitation Annual Maxima

As shown in Figure 2, epistemic uncertainty in the identification of the regional probability distribution is one of the greatest contributors to the total uncertainty and uncertainty bounds for point and watershed PF. A practical approach to modeling the uncertainty in identification of the regional probability distribution is to take advantage of the flexibility of the four-parameter Kappa distribution. L-moment ratio, L-skewness, and L-kurtosis pairings for homogeneous sub-regions can be used to identify the best-fit *h* parameter. One practical approach is to adopt *h* to the nearest 0.05 increment. For this reason, the specific four-parameter Kappa distribution with a fixed second shape parameter *h* can now be treated as a three-parameter distribution with a fixed relationship between L-skewness and L-kurtosis. This approach can be visualized as a unique curve on the LMRD for the best-fit *h* parameter that generally parallels the GEV curve (Figure 4). Consequently, modeling of epistemic uncertainty in regional L-skewness and L-kurtosis yields a bivariate Normal distribution (like Figure 5) centered about the L-moment ratio curve for the best-fit *h* parameter consistent with the sampling variability observed in the original dataset.

The use of a variable *h* parameter to represent a form of model structure uncertainty offers flexibility in describing the behavior of a finite sample and its incomplete convergence to the theoretical distribution of its extremes. However, this flexibility exposes the potential for overfit if not credibly estimated. The regional approach to estimating *h* avoids fitting to small samples where overfit occurs most often, and a limit on the parameter uncertainty is rooted in the theory of extremes.

While other discussions of the limiting law of precipitation extremes, such as Papalexiou and Koutsoyiannis (2013), focus on which of the three GEV subtypes best describes the annual maximum of daily-duration rainfall, the results here show that the GEV subtype is best used as a limiting condition based on the characteristics of the parent population. In addition, incomplete convergence to the extreme value distribution is to be represented using the second Kappa shape parameter *h*. Gumbel Convergence Theory establishes the GEV distribution as the limiting relationship on the LMRD and therefore, sampling for epistemic uncertainty is restricted to the parameter space below the GEV curve on the LMRD for parent populations in that region.

Conversely, an alternative parameter uncertainty estimation scheme invokes the parametric bootstrap, and this scheme is employed as a method for examining the impact of parameter uncertainty on rare quantile inference (Karlovits et al., 2017). When using this procedure, it would be prudent to reject candidate Kappa distribution re-fits which produce an *h* parameter value that lies above the GEV ($h = 0$) line on the LMRD for parent distributions below the line. Utilizing this scheme may affect the estimate of exceedance probability for design depths of precipitation by potentially altering the shape of the confidence limits at remote frequencies.

These findings have the greatest effect on projects in arid, semi-arid, and sub-humid climates where fewer storms per year will result in the regional probability distribution being further below the GEV distribution on the LMRD. This situation will result in more benign quantile estimates for extreme AEPs than would be produced by the adoption of the GEV distribution, the effect of which can be seen in Figure 16. In addition, restriction of distribution choices to below the GEV on the LMRD in the uncertainty analysis will result in smaller quantile estimates for the mean-frequency curve and upper 90% uncertainty bound. Both situations combine to reduce unrealistically large quantile estimates for extreme events that are important considerations in hydrologic risk analysis and RIDM.

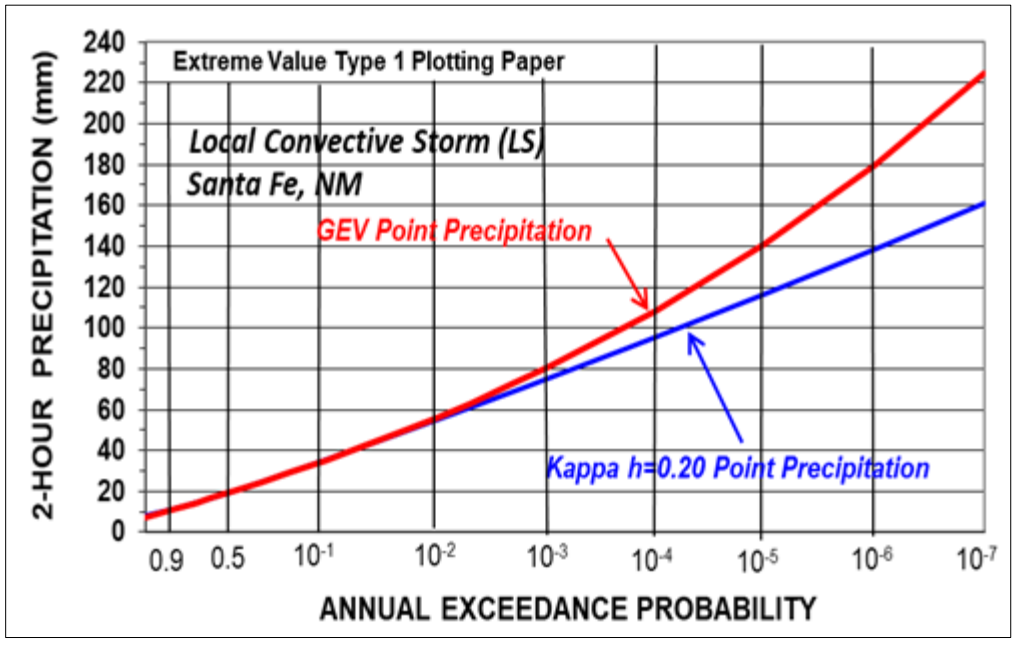

Figure 16. Moderation of extreme quantile Annual Exceedance Probability (AEP) estimates when adopting the Kappa distribution over the Generalized Extreme Value (GEV).

Summary and Conclusions

The recent implementation of storm typing in assembling precipitation annual maxima datasets for regional PF analysis has led to examination of Gumbel's extreme value theory in light of L-moments technology. Observations for large-area regional precipitation-frequency analyses show that extreme precipitation data that are meteorologically-homogenous have properties predicted by classical extreme value theory. Maxima of these homogenous populations demonstrate convergence to the GEV distribution from below the GEV curve on the LMRD for durations representing individual storm events. These maxima are most often drawn from GPA or near-GPA parent distributions. These two results are predicted by the first and second extreme value theorems, respectively.

Annual maxima from these homogenous populations tend to show incomplete convergence to the GEV distribution due to the limited frequency of these storm events occurring per year. Moreover, Monte Carlo simulations demonstrated the rate and trajectory of convergence of various populations as well as the asymptotic limit at the GEV distribution, which for many parent populations, occurs at a very large number of events per year. The four-parameter Kappa distribution allows for regionally-based modeling of precipitation extremes that exhibit varying levels of convergence to the asymptotic result suggested by classical extreme value theory.

As risk-informed decision-making matures and uncertainty is better incorporated into the decision-making process for water infrastructure risk assessments, the quantification of uncertainties in the hazard modeling process become more important. The convergence theory, outlined above, offers guidance to hazard modelers regarding the selection of the regional distribution for precipitation-frequency studies as well as the expression of parameter uncertainty, which when estimated consistently across studies, contributes to the risk-informed decision-making process in a meaningful way.

Acknowledgments, Samples, and Data

Dr. Schaefer's work was performed pro bono. Mr. Karlovits' work was funded through the USACE Flood and Coastal Systems Research and Development program. The authors acknowledge the assistance of MetStat, Inc. in assembling the peaks-over-threshold datasets for the various storm types. The data used to produce the figures and tables can be made available from the following repository: https://github.com/ejgumbel/PFHA_Paper

References

Alexander, G.N. (1963). Using the probability of storm transposition for estimation the frequency of rare flood events. *Journal of Hydrology*, Vol. 1, pp 46-57. https://doi.org/10.1016/0022-1694(63)90032-5

Balkema, A.A., & de Haan, L. (1974). Residual life time at great age. *The Annals of Probability*, 2(5), 792-804. https://www.jstor.org/stable/2959306

Carney, S., Schaefer, M., Barker, B., Parzybok, T., McIntosh, J., & Micheletty, P. (2018). TVA probabilistic flood hazards analysis overview. Prepared for the Tennessee Valley Authority (TVA) Probabilistic Flood Hazards Analysis study. http://www.mgsengr.com/damsafetyfiles/TVA_Point%20Precipitation-Frequency_2015-03-02_Release.pdf

Chow, V.T., Maidment, D.R., & Mays, L.W. (1988). *Applied hydrology*. New York: McGraw-Hill.

Embrechts, P., Klüppelberg, C., & Mikosch, T. (1997). Modelling extremal events: For insurance and finance. *Stochastic Modelling and Applied Probability*, (Vol. 33). Berlin, Germany: Springer-Verlag. https://doi.org/10.1007/978-3-642-33483-2

Fontaine, T.A., & Potter, K.W. (1989). Estimation probabilities of extreme rainfalls, journal of hydraulics engineering. *American Society of Civil Engineers*, 115(11), 1562-1757. https://doi.org/10.1061/(ASCE)0733-9429(1989)115:11(1562)

Foufoula-Georgiou, E. (1989). A probability storm transposition approach for estimating exceedance probabilities of extreme precipitation depths. *Water Resources Research*, 25(5), 799-815. https://doi.org/10.1029/WR025i005p00799

Fisher, R.A., & Tippett, L.H.C. (1928). Limiting forms of the frequency distribution of the largest or smallest member of a sample. *Mathematical Proceedings of the Cambridge Philosophical Society*, 24(2), 180-190. https://doi.org/10.1017/S0305004100015681

Fréchet, M. (1927). Sur la loi de probabilité de l'écart maximum. *Rocznik Polskie Towarzystwo Matematicze (Annales de la Société Polonaise de Mathématique* (Cracow)), 6, 93-116. http://fbc.pionier.net.pl/id/oai:rcin.org.pl:18111

Gnedenko, B.V., (1943). Sur la distribution limité du terme d'une série aléatoire. *Ann. Math.*, 44, 423-453. https://doi.org/10.2307/1968974

Goldie, C.M., & Resnick, S. (1988). Distributions that are both subexponential and in the domain of attraction of an extreme-value distribution. *Advances in Applied Probability*, 20(4), 706-718. https://doi.org/10.2307/1427356

Gumbel, E.J. (1935). Les valeurs extrêmes des distributions statistiques. *Annales de l'institut Henri Poincaré*, 5, 115-158. http://www.numdam.org/item?id=AIHP_1935__5_2_115_0

Gumbel, E.J. (1958). *Statistics of Extremes*. New York: Columbia University Press.

Hosking, J.R.M. (1990). L-moments: Analysis and estimation of distributions using linear combinations of order statistics. *Journal Royal Statistical Society*, *Series B*, 52, 105-124. https://www.jstor.org/stable/2345653

Hosking, J.R.M. (1994). The four-parameter kappa distribution. *IBM Journal of Research and Development*, 38(3), 251-258. https://doi.org/10.1147/rd.383.0251

Hosking, J.R.M., & Wallis, J.R. (1987). Parameter and quantile estimation for the generalized Pareto distribution. *Technometrics*, 29(3), 339-349. https://www.jstor.org/stable/1269343

Hosking, J.R.M., & Wallis, J.R. (1997). *Regional frequency analysis: An approach based on L-moments*. New York: Cambridge University Press.

Hosking, J.R.M., Wallis, J.R., & Wood, E.F. (1985). Estimation of the generalized extreme-value distribution by the method of probability-weighted moments. *Technometrics*, 27(3), 251-261. https://doi.org/10.1080/00401706.1985.10488049

Jenkinson, A.F. (1955). The frequency distribution of the annual maximum (or minimum) values of meteorological elements. *Quarterly Journal of Royal Meteorological Society*, 81(348), 158-171. https://doi.org/10.1002/qj.49708134804

Jenkinson, A.F. (1969). Estimation of maximum floods. *World Meteorological Organization* WMO-No.233.TP.126 (Technical Note, 98, pp. 183-227). Geneva, Switzerland: World Meteorological Organization. https://library.wmo.int/doc_num.php?explnum_id=3444

Karlovits, G.S., Otero, W., & Brown, W.A. (2017). Willamette basin regional 72-hour precipitation frequency analysis. Prepared for U.S. Army Corps of Engineers Risk Management Center (RMC-TR-2017-05), Lakewood, CO: Risk Management Center, Western Division.

L-RAP, (2005). *L-moments regional analysis program*, MGS Software LLC developed by M.G. Schaefer and B.L. Barker. Olympia WA: MGS Engineering Consultants, Inc.

Madsen, H., Rasmussen, P.F., & Rosbjerg, D. (1997). Comparison of annual maximum series and partial duration series methods for modeling extreme hydrologic events: 1. At-site modeling. *Water Resources Research*, 33(4), 747-757. https://doi.org/10.1029/96WR03848

MetStat, MGS Engineering Consultants. (2018a). Trinity river hydrologic hazards project task 3 report – regional extreme precipitation-frequency analysis for the trinity river basin. Prepared for U.S. Army Corps of Engineers, Risk Management Center, May 2018. Lakewood, CO: Risk Management Center, Western Division.

MetStat, MGS Engineering Consultants. (2018b). Colorado-New Mexico regional extreme precipitation study, summary report volume iii, regional precipitation-frequency estimation. Prepared for Colorado and New Mexico Dam Safety Programs, Nov 2018. Lakewood, CO: Risk Management Center, Western Division.

MGS Engineering Consultants, MetStat, Applied Climate Services, & Riverside Technology. (2015). Regional precipitation-frequency analyses for mid-latitude cyclones, mesoscale storms with embedded convection, local storms and tropical storm remnant storm types in the Tennessee valley watershed. Prepared for Tennessee Valley Authority (TVA), Knoxville, TN. http://www.mgsengr.com/damsafetyfiles/TVA_Point%20Precipitation-Frequency_2015-03-02_Release.pdf

Nathan, R.J., Weinmann, E.M., & Hill, P. (2003). Use of Monte Carlo simulation to estimate the expected probability of large to extreme floods. In M.J. Boyd, J.E. Ball, M.K. Babister, & J. Green (Eds.), *28th International Hydrology and Water Resources Symposium: About Water; Symposium Proceedings* (1.105-1.112). Barton, A.C.T.: Institution of Engineers, Australia. https://search.informit.com.au/documentSummary;dn=350910043129567;res=IELENG

Nathan, R., Jordan, P., Scorah, M., Lang, S., Kuczera, G., Schaefer, M., & Weinmann E. (2016). Estimating the exceedance probability of probable maximum precipitation. *Journal of Hydrology*, 543B, 706-720. https://doi.org/10.1016/j.jhydrol.2016.10.044

Nunez, J.H., Verbist, K., Wallis, J.R., Schaefer, M.G., Morales, L., & Cornelis, W.M. (2011). Regional frequency analysis for mapping drought events in north-central Chile. *Journal of Hydrology*, 405(4-5), 352-366. https://doi.org/10.1016/j.jhydrol.2011.05.035

Papalexiou, S.M., & Koutsoyiannis, D. (2013). Battle of extreme value distributions: A global survey on extreme daily rainfall. *Water Resources Research*, 49(1), 187-201. https://doi.org/10.1029/2012WR012557

Pickands, J. (1975). Statistical inference using extreme order statistics. *The Annals of Statistics*, 3(1), 119-131. https://doi.org/10.1214/aos/1176343003

Resnick, S.I. (1986). Point Processes, Regular Variation and Weak Convergence. *Advances in Applied Probability*, 18(1), 66-138. https://www.jstor.org/stable/1427239

Resnick, S.I. (2007). *Heavy-Tail Phenomena: Probabilistic and Statistical Modeling*. New York, NY: Springer-Verlag. https://www.springer.com/us/book/9780387242729

Schaefer, M.G., & Barker, B.L. (2005). Stochastic modeling of extreme floods on the American River at Folsom Dam flood-frequency curve extension. MGS Engineering Consultants, Inc., prepared for U.S. Army Corps of Engineers, Hydrologic Engineering Center, Davis CA. https://www.hec.usace.army.mil/publications/ResearchDocuments/RD-48.pdf

Schaefer, M.G., Wallis, J.R., Taylor, G.H., & Parzybok, T.W. (2016). Technical memorandum, regional precipitation-frequency analysis using the climate region method for application in analyses of extreme precipitation and floods. Prepared for Colorado-New Mexico Regional Extreme Precipitation Study, 2016. https://metstat.com/papers_presentations/TM_RegionalPrecipAnalysis_ClimateRegionMethod_SWT_2019May07.pdf

Schaefer, M.G. (2017a). Technical memorandum, algorithm for stochastic storm generation of watershed precipitation-frequency relationships for synoptic scale mid-latitude cyclone and tropical storm remnant storm types. Prepared for Tennessee Valley Authority, Knoxville, TN. https://metstat.com/papers_presentations/TM_StochasticStormGenerationMLC_20170119_Final.pdf

Schaefer, M.G. (2017b). Technical memorandum, watershed precipitation-frequency development via stochastic storm transposition for geographically fixed areas for the mesoscale storm with embedded convection storm type (move-the-earth algorithm). Prepared for Tennessee Valley Authority, Knoxville, TN. https://metstat.com/papers_presentations/TM_StochasticMove-the-Earth_MEC_20181030_Final.pdf

SEFM. (1998). Stochastic event flood model user's manual, MGS Software LLC developed by M.G. Schaefer and B.L. Barker (2001, 2009, 2015, & 2019). Olympia WA: MGS Engineering Consultants, Inc. http://www.mgsengr.com/SEFM/Download/SEFM_TechnicalSupportManual_March2018.pdf

Smith, C.H., Karlovits, G.S., Moses, D.W., & Nelson, A.G. (2015). Herbert Hoover Dike hydrologic hazard assessment. Prepared for U.S. Army Corps of Engineers, Jacksonville District, Jacksonville, FL.

Stedinger, J.R., Vogel, R.M., & Foufoula-Georgiou, E. (1993). Frequency analysis of extreme events. In D.R. Maidment (Ed.), *Handbook of Hydrology*, (Chapter 18). New York: McGraw-Hill.

Vogel, R.M., & Fennessey, N.M. (1993). L-moment diagrams should replace product-moment diagrams. *Water Resources Research*, 29, 1745-52. https://doi.org/10.1029/93WR00341

Technical Paper Series

TP-1 Use of Interrelated Records to Simulate Streamflow
TP-2 Optimization Techniques for Hydrologic Engineering
TP-3 Methods of Determination of Safe Yield and Compensation Water from Storage Reservoirs
TP-4 Functional Evaluation of a Water Resources System
TP-5 Streamflow Synthesis for Ungaged Rivers
TP-6 Simulation of Daily Streamflow
TP-7 Pilot Study for Storage Requirements for Low Flow Augmentation
TP-8 Worth of Streamflow Data for Project Design - A Pilot Study
TP-9 Economic Evaluation of Reservoir System Accomplishments
TP-10 Hydrologic Simulation in Water-Yield Analysis
TP-11 Survey of Programs for Water Surface Profiles
TP-12 Hypothetical Flood Computation for a Stream System
TP-13 Maximum Utilization of Scarce Data in Hydrologic Design
TP-14 Techniques for Evaluating Long-Tem Reservoir Yields
TP-15 Hydrostatistics - Principles of Application
TP-16 A Hydrologic Water Resource System Modeling Techniques
TP-17 Hydrologic Engineering Techniques for Regional Water Resources Planning
TP-18 Estimating Monthly Streamflows Within a Region
TP-19 Suspended Sediment Discharge in Streams
TP-20 Computer Determination of Flow Through Bridges
TP-21 An Approach to Reservoir Temperature Analysis
TP-22 A Finite Difference Methods of Analyzing Liquid Flow in Variably Saturated Porous Media
TP-23 Uses of Simulation in River Basin Planning
TP-24 Hydroelectric Power Analysis in Reservoir Systems
TP-25 Status of Water Resource System Analysis
TP-26 System Relationships for Panama Canal Water Supply
TP-27 System Analysis of the Panama Canal Water Supply
TP-28 Digital Simulation of an Existing Water Resources System
TP-29 Computer Application in Continuing Education
TP-30 Drought Severity and Water Supply Dependability
TP-31 Development of System Operation Rules for an Existing System by Simulation
TP-32 Alternative Approaches to Water Resources System Simulation
TP-33 System Simulation of Integrated Use of Hydroelectric and Thermal Power Generation
TP-34 Optimizing flood Control Allocation for a Multipurpose Reservoir
TP-35 Computer Models for Rainfall-Runoff and River Hydraulic Analysis
TP-36 Evaluation of Drought Effects at Lake Atitlan
TP-37 Downstream Effects of the Levee Overtopping at Wilkes-Barre, PA, During Tropical Storm Agnes
TP-38 Water Quality Evaluation of Aquatic Systems
TP-39 A Method for Analyzing Effects of Dam Failures in Design Studies
TP-40 Storm Drainage and Urban Region Flood Control Planning
TP-41 HEC-5C, A Simulation Model for System Formulation and Evaluation
TP-42 Optimal Sizing of Urban Flood Control Systems
TP-43 Hydrologic and Economic Simulation of Flood Control Aspects of Water Resources Systems
TP-44 Sizing Flood Control Reservoir Systems by System Analysis
TP-45 Techniques for Real-Time Operation of Flood Control Reservoirs in the Merrimack River Basin
TP-46 Spatial Data Analysis of Nonstructural Measures
TP-47 Comprehensive Flood Plain Studies Using Spatial Data Management Techniques
TP-48 Direct Runoff Hydrograph Parameters Versus Urbanization
TP-49 Experience of HEC in Disseminating Information on Hydrological Models
TP-50 Effects of Dam Removal: An Approach to Sedimentation
TP-51 Design of Flood Control Improvements by Systems Analysis: A Case Study
TP-52 Potential Use of Digital Computer Ground Water Models
TP-53 Development of Generalized Free Surface Flow Models Using Finite Element Techniques
TP-54 Adjustment of Peak Discharge Rates for Urbanization
TP-55 The Development and Servicing of Spatial Data Management Techniques in the Corps of Engineers
TP-56 Experiences of the Hydrologic Engineering Center in Maintaining Widely Used Hydrologic and Water Resource Computer Models
TP-57 Flood Damage Assessments Using Spatial Data Management Techniques
TP-58 A Model for Evaluating Runoff-Quality in Metropolitan Master Planning
TP-59 Testing of Several Runoff Models on an Urban Watershed
TP-60 Operational Simulation of a Reservoir System with Pumped Storage
TP-61 Technical Factors in Small Hydropower Planning
TP-62 Flood Hydrograph and Peak Flow Frequency Analysis
TP-63 HEC Contribution to Reservoir System Operation
TP-64 Determining Peak-Discharge Frequencies in an Urbanizing Watershed: A Case Study
TP-65 Feasibility Analysis in Small Hydropower Planning
TP-66 Reservoir Storage Determination by Computer Simulation of Flood Control and Conservation Systems
TP-67 Hydrologic Land Use Classification Using LANDSAT
TP-68 Interactive Nonstructural Flood-Control Planning
TP-69 Critical Water Surface by Minimum Specific Energy Using the Parabolic Method
TP-70 Corps of Engineers Experience with Automatic Calibration of a Precipitation-Runoff Model
TP-71 Determination of Land Use from Satellite Imagery for Input to Hydrologic Models

TP-72 Application of the Finite Element Method to Vertically Stratified Hydrodynamic Flow and Water Quality
TP-73 Flood Mitigation Planning Using HEC-SAM
TP-74 Hydrographs by Single Linear Reservoir Model
TP-75 HEC Activities in Reservoir Analysis
TP-76 Institutional Support of Water Resource Models
TP-77 Investigation of Soil Conservation Service Urban Hydrology Techniques
TP-78 Potential for Increasing the Output of Existing Hydroelectric Plants
TP-79 Potential Energy and Capacity Gains from Flood Control Storage Reallocation at Existing U.S. Hydropower Reservoirs
TP-80 Use of Non-Sequential Techniques in the Analysis of Power Potential at Storage Projects
TP-81 Data Management Systems of Water Resources Planning
TP-82 The New HEC-1 Flood Hydrograph Package
TP-83 River and Reservoir Systems Water Quality Modeling Capability
TP-84 Generalized Real-Time Flood Control System Model
TP-85 Operation Policy Analysis: Sam Rayburn Reservoir
TP-86 Training the Practitioner: The Hydrologic Engineering Center Program
TP-87 Documentation Needs for Water Resources Models
TP-88 Reservoir System Regulation for Water Quality Control
TP-89 A Software System to Aid in Making Real-Time Water Control Decisions
TP-90 Calibration, Verification and Application of a Two-Dimensional Flow Model
TP-91 HEC Software Development and Support
TP-92 Hydrologic Engineering Center Planning Models
TP-93 Flood Routing Through a Flat, Complex Flood Plain Using a One-Dimensional Unsteady Flow Computer Program
TP-94 Dredged-Material Disposal Management Model
TP-95 Infiltration and Soil Moisture Redistribution in HEC-1
TP-96 The Hydrologic Engineering Center Experience in Nonstructural Planning
TP-97 Prediction of the Effects of a Flood Control Project on a Meandering Stream
TP-98 Evolution in Computer Programs Causes Evolution in Training Needs: The Hydrologic Engineering Center Experience
TP-99 Reservoir System Analysis for Water Quality
TP-100 Probable Maximum Flood Estimation - Eastern United States
TP-101 Use of Computer Program HEC-5 for Water Supply Analysis
TP-102 Role of Calibration in the Application of HEC-6
TP-103 Engineering and Economic Considerations in Formulating
TP-104 Modeling Water Resources Systems for Water Quality
TP-105 Use of a Two-Dimensional Flow Model to Quantify Aquatic Habitat
TP-106 Flood-Runoff Forecasting with HEC-1F
TP-107 Dredged-Material Disposal System Capacity Expansion
TP-108 Role of Small Computers in Two-Dimensional Flow Modeling
TP-109 One-Dimensional Model for Mud Flows
TP-110 Subdivision Froude Number
TP-111 HEC-5Q: System Water Quality Modeling
TP-112 New Developments in HEC Programs for Flood Control
TP-113 Modeling and Managing Water Resource Systems for Water Quality
TP-114 Accuracy of Computer Water Surface Profiles - Executive Summary
TP-115 Application of Spatial-Data Management Techniques in Corps Planning
TP-116 The HEC's Activities in Watershed Modeling
TP-117 HEC-1 and HEC-2 Applications on the Microcomputer
TP-118 Real-Time Snow Simulation Model for the Monongahela River Basin
TP-119 Multi-Purpose, Multi-Reservoir Simulation on a PC
TP-120 Technology Transfer of Corps' Hydrologic Models
TP-121 Development, Calibration and Application of Runoff Forecasting Models for the Allegheny River Basin
TP-122 The Estimation of Rainfall for Flood Forecasting Using Radar and Rain Gage Data
TP-123 Developing and Managing a Comprehensive Reservoir Analysis Model
TP-124 Review of U.S. Army corps of Engineering Involvement With Alluvial Fan Flooding Problems
TP-125 An Integrated Software Package for Flood Damage Analysis
TP-126 The Value and Depreciation of Existing Facilities: The Case of Reservoirs
TP-127 Floodplain-Management Plan Enumeration
TP-128 Two-Dimensional Floodplain Modeling
TP-129 Status and New Capabilities of Computer Program HEC-6: "Scour and Deposition in Rivers and Reservoirs"
TP-130 Estimating Sediment Delivery and Yield on Alluvial Fans
TP-131 Hydrologic Aspects of Flood Warning - Preparedness Programs
TP-132 Twenty-five Years of Developing, Distributing, and Supporting Hydrologic Engineering Computer Programs
TP-133 Predicting Deposition Patterns in Small Basins
TP-134 Annual Extreme Lake Elevations by Total Probability Theorem
TP-135 A Muskingum-Cunge Channel Flow Routing Method for Drainage Networks
TP-136 Prescriptive Reservoir System Analysis Model - Missouri River System Application
TP-137 A Generalized Simulation Model for Reservoir System Analysis
TP-138 The HEC NexGen Software Development Project
TP-139 Issues for Applications Developers
TP-140 HEC-2 Water Surface Profiles Program
TP-141 HEC Models for Urban Hydrologic Analysis
TP-142 Systems Analysis Applications at the Hydrologic Engineering Center
TP-143 Runoff Prediction Uncertainty for Ungauged Agricultural Watersheds
TP-144 Review of GIS Applications in Hydrologic Modeling

TP-145 Application of Rainfall-Runoff Simulation for Flood Forecasting
TP-146 Application of the HEC Prescriptive Reservoir Model in the Columbia River Systems
TP-147 HEC River Analysis System (HEC-RAS)
TP-148 HEC-6: Reservoir Sediment Control Applications
TP-149 The Hydrologic Modeling System (HEC-HMS): Design and Development Issues
TP-150 The HEC Hydrologic Modeling System
TP-151 Bridge Hydraulic Analysis with HEC-RAS
TP-152 Use of Land Surface Erosion Techniques with Stream Channel Sediment Models
TP-153 Risk-Based Analysis for Corps Flood Project Studies - A Status Report
TP-154 Modeling Water-Resource Systems for Water Quality Management
TP-155 Runoff simulation Using Radar Rainfall Data
TP-156 Status of HEC Next Generation Software Development
TP-157 Unsteady Flow Model for Forecasting Missouri and Mississippi Rivers
TP-158 Corps Water Management System (CWMS)
TP-159 Some History and Hydrology of the Panama Canal
TP-160 Application of Risk-Based Analysis to Planning Reservoir and Levee Flood Damage Reduction Systems
TP-161 Corps Water Management System - Capabilities and Implementation Status
TP-162 Watershed Impact Analysis: Effects of Urbanization on the Cottonwood Creek, CA Watershed - Sacramento & San Joaquin River Basins Comprehensive Study
TP-163 Identifying the Probability Distribution of Precipitation Annual Maxima for Probabilistic Flood Hazard Analysis: Implications of Gumbel's Extreme Value Theory